Journal of Membrane Science 665 (2023) 121114

Contents lists available at ScienceDirect

Journal of Membrane Science

journal homepage: www.elsevier.com/locate/memsci

Transport mechanisms in electrodialysis: The effect on selective ion transport in multi-ionic solutions

Selin Ozkul [a], Jonathan J. van Daal [a], Norbert J.M. Kuipers [b], Roel J.M. Bisselink [b], Harry Bruning [a], Jouke E. Dykstra [a,*], Huub H.M. Rijnaarts [a]

[a] Environmental Technology, Wageningen University & Research, Bornse Weilanden 9, 6708 WG, Wageningen, the Netherlands
[b] Food and Biobased Research, Wageningen University & Research, Bornse Weilanden 9, 6708 WG, Wageningen, the Netherlands

ARTICLE INFO

Keywords:
Electrodialysis
Ion selectivity
Ion transport modelling
Membrane characterization
Water transport

ABSTRACT

Water reuse is one of the possible solutions to prevent depletion of freshwater resources; however, it is often limited by the accumulation of specific ions in the recirculating water. Ion selective desalination technologies can increase the potential for water reuse. Electrodialysis is a water treatment technology that is able to selectively remove ions from water. In order to enhance and further develop the selectivity of the process, a fundamental understanding of the various mechanisms governing multi-ion transport in electrodialysis is essential. In the present study, a theoretical model for multi-ionic (Na^+ and K^+) mass transport in electrodialysis was developed including ion-water and ion-membrane frictions, and water transport. General properties and the selectivity of ion exchange membranes towards K^+ over Na^+ ions were experimentally determined and included in the model. The theory was successfully validated for ion flux through the membranes, ion concentrations in the solutions, and water transport by comparing theory with batch-mode electrodialysis experiments. Contributions of different ion transport mechanisms to the selective transport of Na^+ and K^+ ions were evaluated by model calculations. It was found that electromigration has the largest contribution to ion transport followed by convection, and that diffusion controls the selectivity of ion transport in electrodialysis under constant voltage operation.

1. Introduction

Water reuse in closed cycle systems gains more importance in various sectors due to increasing demand for freshwater and due to stricter regulations. However, continuous use of water in closed cycle systems can result in accumulation of harmful salt ions, such as Na^+, which decreases the recirculation water quality and limits the possibilities for re-use applications [1,2]. In addition, the discharge of low-quality recirculation water results in a loss of water and valuable compounds, such as K^+. In order to increase the potential for water re-use in closed water cycle systems, it is necessary to develop desalination technologies that selectively remove undesirable ions and retain desirable ions in solution.

One of the most commonly applied desalination technologies is electrodialysis (ED), which is an electrically driven membrane-based desalination process mainly used for brackish water desalination or water reuse [3,4]. A conventional ED unit consists of two electrodes and alternatingly placed anion exchange membranes (AEM) and cation exchange membranes (CEM), see Fig. 1. A spacer gasket is placed between the membranes to create flow channels [5,6]. When an electrical voltage is applied over the electrodes, ions move towards the oppositely charged electrodes, and are blocked by the equally charged membranes [7–9]. Due to the arrangement of ion-selective membranes, the concentration of ions either decreases or increases in each alternate flow channel (Fig. 1). Unlike membrane-based desalination technologies that separate ions mainly based on their size, in ED ions are selectively transported depending on ionic charge, the operational conditions (applied current, water flowrate, ionic content of the water, etc.) and the membrane characteristics (thickness, fixed charge density, ion affinity, etc.) [10]. Several process parameters can be tuned to achieve ion-selective transport in ED.

Various studies have been performed to evaluate monovalent and divalent ion selectivity of ED considering the system operational conditions, such as applied current density [11–13] and temperature [13,14], and modified membranes, such as monovalent selective membranes [15–18]. However, selective separation of ions with the same valency is

* Corresponding author.
E-mail address: jouke.dykstra@wur.nl (J.E. Dykstra).

https://doi.org/10.1016/j.memsci.2022.121114
Received 29 March 2022; Received in revised form 3 August 2022; Accepted 19 October 2022
Available online 23 October 2022

more complicated due to similar physical-chemical properties of the ions. Only a few studies have been conducted to explore the selectivity of different monovalent ions in ED, mainly using modified ion exchange membranes. Sata et al. [19], Li et al. [20] and Mubita et al. [21] have investigated the effect of membrane hydrophilicity on the selectivity of monovalent anions, and they have reported that the selectivity of anion exchange membranes can be enhanced towards ions with lower hydration energy by increasing the hydrophobicity of the membranes. Qian et al. [22] and Yang et al. [23] have studied the effect of using crown ether doped membranes on specific monovalent ion removal, which allows membranes to selectively bind and immobilize specific monovalent ions, affecting the transport properties of the membranes. They have reported that the selective removal of specific monovalent cations can be achieved mainly based on the size and mobility of the ions due to the compact modified layer formed inside the membranes [22,23].

Studying ion transport mechanisms that take place in ED is key to understand the selectivity of the system. An ED model describing different ion transport mechanisms, such as electromigration, diffusion and convection, would provide a better understanding of preferential ion transport through ion exchange membranes and would enable further improvement of ED technology for ion-selective removal. To describe ion and water transport in ED, the specific ion interactions in membranes with other ions in solution must be considered, as well as the interactions with charged membrane components that are regarded as constituents of a complex solution mixture [24–27]. In several studies, simplifications are made, and only a single effective diffusion coefficient for each ion inside the membrane that is a certain combination of the ionic interaction coefficients is considered [28,29]. Several theoretical studies have been conducted to evaluate ion transport in ED, however, these studies have limitations to evaluate ion selectivity due to assumptions such as having only one type of (counter) ion in the solution [6,26,27,30–33], disregarding specific properties of the AEMs and CEMs [24,27,31,32,34–36], and neglecting ion transport due to water transport through the membranes [31,35].

In the present work, we aim to improve the understanding of selective ion transport in ED (Fig. 1) by experimental and theoretical studies. For that purpose, we developed a theoretical model to describe individual ion transport through the membranes for multi-ionic solutions in an ED stack. We experimentally determined the membrane and ion specific properties, such as affinity and diffusion coefficients of ions inside the membrane. We conducted batch-mode ED experiments using single salt (Na^+) and multi-ionic solutions (Na^+ and K^+) in order to validate the theory. In addition, we provided theoretical calculations for the contribution of different transport mechanisms on individual ion transport, and ion selective removal in multi-ionic solutions.

2. Theory

The theoretical framework was developed for binary mixtures, considering Na^+ and K^+ as target ions, including ion-membrane, membrane-water and ion-water frictions; ion-ion frictions were neglected. Water transport was evaluated considering the membrane-water and ion-water frictions, and the ion concentration differences over the membranes [28]. The membranes were considered as homogeneous, and ion transport was evaluated in the x-direction inside the membranes. In the entire system complete dissociation of the ions was assumed. Also, ideal thermodynamics were considered, which means that ionic concentrations were used for calculations rather than activities. The concentrate and diluate channels were assumed to be ideally mixed, and the diffusion boundary layer concentration gradients were neglected. This assumption is considered to be valid for the batch ED system we study, considering the operational conditions, such as very high flow rates in the ED cell, which improves mixing in the channels.

The computational domain of the theoretical framework is the repeating unit of the ED cell, which includes an AEM, a concentrate channel, a CEM and a diluate channel. Additionally, we include the concentrate and diluate reservoirs. The electrode compartments were not included in the theory. Including the complete cell in the domain allows to model both membranes asymmetrically, and to introduce different properties of the AEM and CEM into the model such as

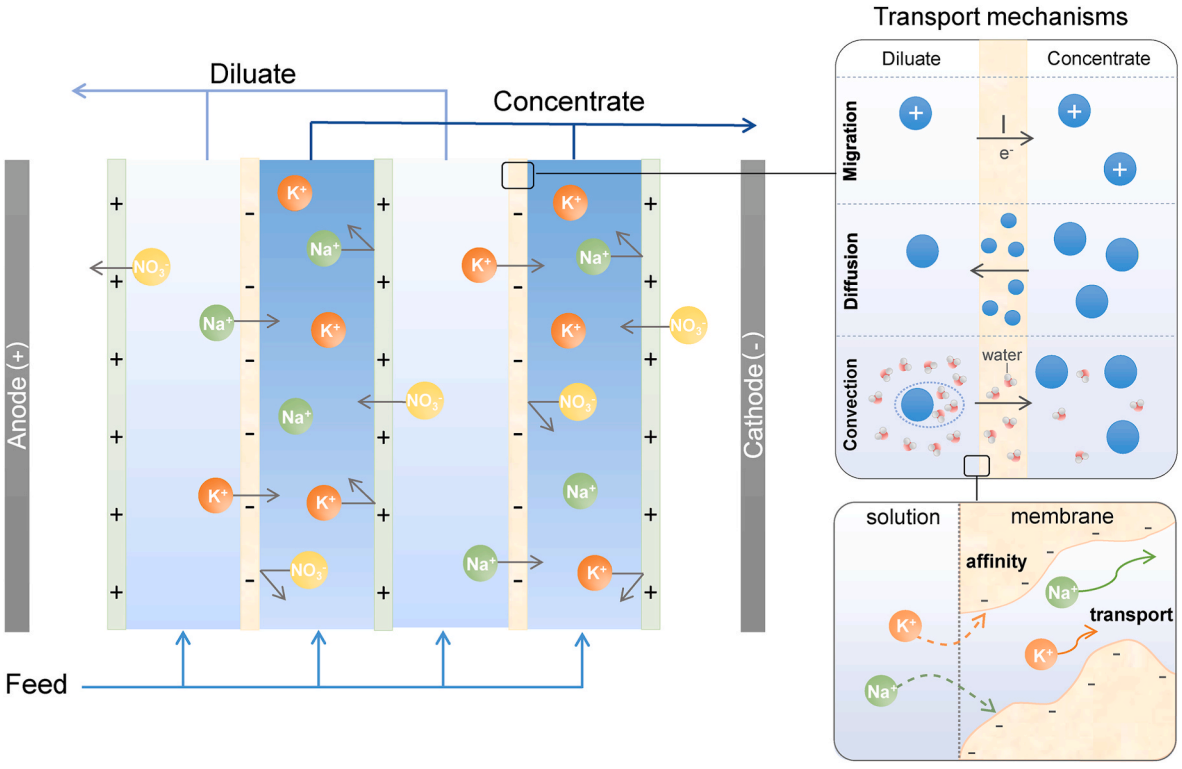

Fig. 1. Schematic description of electrodialysis, the ion transport mechanisms, and the partitioning of ions at the membrane-solution interface.

thickness, fixed charge density, and the membrane-water friction coefficient. The theoretical framework is described in three parts in the present study: membranes, flow channels and reservoirs, and boundary and initial conditions.

2.1. Membranes

Ion transport across the membrane was evaluated starting from a force balance, which describes the total driving force acting on an ion based on the gradient of the chemical potential [37]. Inside the membrane, the concentration and potential gradients in the *y*-direction were assumed to be zero; hence, the derivative of the chemical potential of an ion in the membrane was evaluated in the *x*-direction as,

$$\frac{1}{RT}\frac{\partial \overline{\mu}_i}{\partial x} = -\sum_i f_{i-j}\left(v_i - v_j\right) \tag{1}$$

where $\overline{\mu}_i$ is the chemical potential of an ion (J·mol^{-1}), x is the position inside the membrane (m), R is the ideal gas constant (8.314 J·mol^{-1}·K^{-1}), T is the temperature (K), f_{i-j} is the friction factor (s·m^{-2}) between ion i and phase j, v_i and v_j are the superficial velocities (m·s^{-1}) of ion i and phase j. Subscript j can refer to the fluid, to the membrane or to other ions. The chemical potential of an ion is given by

$$\overline{\mu}_i = \overline{\mu}_{i0} + RT\ln c_{\mathrm{m},i} + RTz_i\phi \tag{2}$$

where $c_{\mathrm{m},i}$ is the ion concentration (mol·L^{-1}) inside the membrane, z_i is the ion valence, F is the Faraday constant (96,485 C·mol^{-1}), and ϕ is the dimensionless electrical potential that can be multiplied by RT/F to calculate the dimensional voltage. By neglecting ion-ion frictions and considering the membrane matrix velocity, v_{m}, as zero, substituting Eq. (2) into Eq. (1) for ion i gives

$$\frac{\partial \ln c_{\mathrm{m},i}}{\partial x} + z_i\frac{\partial \phi}{\partial x} = -\left(f_{i-\mathrm{w}}\left(v_i - v_{\mathrm{w}}\right) + f_{i-\mathrm{m}}v_i\right) \tag{3}$$

where v_{w} is the water velocity, $f_{i-\mathrm{w}}$ and $f_{i-\mathrm{m}}$ are the specific ion-water and ion-membrane friction factors, respectively. The diffusion coefficient of an ion inside the membrane can be defined in terms of the frictions acting on the ion, $D = 1/f$. Considering the ion-water and ion-membrane frictions, the diffusion coefficients of ions inside the membrane can be evaluated as [32]

$$\frac{1}{D_i} = \frac{1}{D_{i-\mathrm{w}}} + f_{i-\mathrm{m}} \tag{4}$$

where D_i is the modified diffusion coefficient (m^2·s^{-1}) of an ion inside the membrane and $D_{i-\mathrm{w}}$ is the ion-water diffusion coefficient inside the membrane. Please note that we leave out index * in symbol D_i, which was used in Ref. [32]. By substituting Eq. (4) into Eq. (3), the ion velocity inside the membrane is given by

$$v_i = \frac{D_i}{D_{i-\mathrm{w}}}v_{\mathrm{w}} - D_i\left(\frac{\partial \ln c_{\mathrm{m},i}}{\partial x} + z_i\frac{\partial \phi}{\partial x}\right) \tag{5}$$

including the ion-water and ion-membrane friction. The ratio $D_i/D_{i-\mathrm{w}}$ is equal to $K_{\mathrm{f},i}$, the hindrance function, which is given by $K_{\mathrm{f},i} = 1/(1 + f_{i-\mathrm{m}}/f_{i-\mathrm{w}})$ and D_i is equal to $D_i = K_{\mathrm{f},i}D_{\mathrm{m},i}$, with $D_{\mathrm{m},i} = 1/f_{i-\mathrm{w}}$ as used in Eq. (83) in Biesheuvel et al. [37]. Inside the membrane, the diffusion coefficient of an ion is lower than the value in free solution due to the interaction of ions with the membrane surface groups, and due to tortuosity and membrane porosity, and is affected differently for each ion [38,39]. The reduction factors were considered in the present model as dimensionless correction factors, and the diffusion coefficients of ions inside the membrane are given by

$$D_i = \frac{D_{i,\infty}}{d_{\mathrm{r},i}} \tag{6}$$

$$D_{i-\mathrm{w}} = \frac{D_{i,\infty}}{d_{\mathrm{r},i-\mathrm{w}}} \tag{7}$$

where $D_{i,\infty}$ is the diffusion coefficient of an ion in free solution, $d_{\mathrm{r},i}$ is the ion specific reduction factor for D_i, and $d_{\mathrm{r},i-\mathrm{w}}$ is the reduction factor for $D_{i-\mathrm{w}}$, which was reported to be between 10 and 20 [32] for which we used $d_{\mathrm{r},i-\mathrm{w}} = 22$ in the present study. Ion fluxes (J_i, mol·m^{-2}·s^{-1}) were evaluated at each position inside the membrane by substituting Eqs. (5)–(7) into $J_i = c_{\mathrm{m},i}v_i$ resulting in

$$J_i = \frac{d_{\mathrm{r},i-\mathrm{w}}}{d_{\mathrm{r},i}}v_{\mathrm{w}}c_{\mathrm{m},i} - \frac{D_{i,\infty}}{d_{\mathrm{r},i}}\left(\frac{\partial c_{\mathrm{m},i}}{\partial x} + z_i c_{\mathrm{m},i}\frac{\partial \phi}{\partial x}\right) \tag{8}$$

which is the extended Nernst-Planck equation including ion-water and ion-membrane friction. Eq. (8) considers the contributions of different ion transport mechanisms, such as convection due to the water flow, diffusion due to the concentration gradient of an ion and electromigration due to the potential gradient across the membrane (Fig. 1).

At each position inside the membrane, we evaluate the mass balance for each individual ion considering the ionic fluxes using

$$\frac{\partial c_{\mathrm{m},i}}{\partial t} = -\frac{\partial J_i}{\partial x} + \Gamma_i \tag{9}$$

where t is time (s), and Γ_i is the chemical formation rate of ions (mol·L^{-1}·s^{-1}), which is considered to be zero for non-reactive ions, such as Na^+, K^+ and NO_3^-. A theoretical description to account for the mass balances when reactive ions are present in solution can be found in recent studies by Dykstra et al. [40], Shocron et al. [41], and Ronen et al. [42].

Local electroneutrality was also considered at each position in the membrane, considering both the charge of the ions and the chemical charge of the membrane, and is given by

$$\sum_i z_i c_{\mathrm{m},i} + \omega X = 0 \tag{10}$$

where ω is the sign of the membrane charge (−1 for CEM and +1 for AEM), X is the fixed charge density of the membrane (mol·L^{-1}), and i runs over all ionic species. We considered the local electroneutrality condition at each position inside the membrane. The ionic current is invariant with position, which is considered in the model using

$$\frac{\partial}{\partial x}\sum_i z_i J_i = 0. \tag{11}$$

In a cell pair, the total ionic flux can be directly linked to the applied external current. In order to calculate the transport rates of ions, the ionic current inside the membrane was related to the applied current density, I (A·m^{-2}), using

$$I = F\sum_i z_i J_i. \tag{12}$$

The water self-ionization equilibrium reaction, $H_2O \leftrightharpoons H^+ + OH^-$, was also taken into account at each position in the membrane. The reaction was considered as infinitely fast, and local chemical equilibrium between H^+ and OH^- ions was assumed, using

$$K_{\mathrm{w}} = [H^+][OH^-] \tag{13}$$

with K_{w} the equilibrium constant of water ($K_{\mathrm{w}} = 10^{-14}$, in unit M^2). Concentration of OH^- ions is expressed in terms of H^+ ions by substituting Eq. (13) into all equations.

Next, we define the water transport through the membrane to be able to calculate the ionic fluxes with Eq. (8). In the present study, ions were considered as point charges and the volume occupied by ions was not considered. Therefore, the water transport resulted by the hydrostatic and osmotic pressure differences across the membrane, and by the ion-water friction (electro-osmosis), was evaluated. The average superficial

water velocity, v_w, was evaluated using (Eq. (1)) by

$$\frac{\partial P^t}{\partial x} = -f_{w-m} v_w - \sum_i \frac{c_{m,i}}{D_{i-w}} (v_w - v_i) \tag{14}$$

where P^t is the total pressure (mol·L^{-1}), which is hydrostatic pressure (P^h) minus osmotic pressure (Π), $P^t = P^h - \Pi$, and f_{w-m} is the friction coefficient between the water and the membrane. Eq. (5) can be substituted into Eq. (14), and the resulting equation can be further simplified by (i) replacing the diffusion coefficient of the ions, D_i, by substituting Eqs. (4), (6) and (7), (ii) evaluating $d_{r,i}$ being an average value of all ions, $d_{r,avg}$, (iii) expressing the sum of all concentrations as the osmotic pressure, and (iv) substituting the electroneutrality condition inside the membrane, Eq. (10), into the resulting equation. More details are provided in the Supplementary Information (SI).

2.2. Flow channels and reservoirs

Diluate and concentrate channels inside the ED stack, and reservoirs containing the solutions that are recirculated through the ED stack during batch-scale operation were also considered to complete the process model. The mass balances were set up over each flow channel considering the water flows in the channels and the ionic fluxes through the membrane as

$$V_c \frac{\partial c_i}{\partial t} = \left(Q_{in} c_{r,i} - Q_{out} c_i\right) \pm A_{mem} \left(J_{i,AEM} - J_{i,CEM}\right) + \Gamma_i \tag{15}$$

where $c_{r,i}$ is the concentration of ions in the reservoir, c_i is the concentration of ions in the flow channel, V_c is the volume (m^3) of the flow channel, Q_{in} is the inflow and Q_{out} is the outflow of the flow channel (m^3·s^{-1}), and A_{mem} is the cross-sectional area of the membrane (m^2). The ionic fluxes, J_i, going in and out of the flow channels at the boundaries were set equal to the fluxes just inside the membrane for each ion. The water outflow for each flow channel was calculated by

$$Q_{out} = Q_{in} \pm A_{mem} \left(v_{w,AEM} - v_{w,CEM}\right) \tag{16}$$

where the water velocities through AEM and CEM were calculated using Eq. (S5) in the SI. The balances over the reservoirs have to include water transport inside the stack as well. The water volume in the reservoirs was calculated for each reservoir using

$$\frac{\partial V_r}{\partial t} = Q_{out} - Q_{in} \tag{17}$$

where V_r is the volume of the reservoir. The mass balance for the reservoir was included in the model, which is given by

$$\frac{\partial V_r c_{r,i}}{\partial t} = Q_{out} c_i - Q_{in} c_{r,i} + \Gamma_i \, . \tag{18}$$

Electroneutrality was also considered in the flow channels and the reservoirs for all ionic species according to

$$\sum_i z_i c_i = 0 \tag{19}$$

$$\sum_i z_i c_{r,i} = 0. \tag{20}$$

Additionally, the water self-ionization equilibrium, given by Eq. (13), was substituted into all equations.

2.3. Boundary and initial conditions

Boundary conditions were considered in order to relate the concentration of ions in the flow channels to the concentrations inside the membrane at the membrane-solution interface. Due to the fixed charge of the membrane, a potential difference is observed between the bulk solution in the flow channels and the membrane solution. This potential difference, the Donnan potential, occurs at both sides of the membrane and results in a higher counterion and a lower co-ion concentration just inside the membrane compared to the bulk solution [43]. The Donnan potential can be derived from the chemical potential (Eq. (2)). At equilibrium, the chemical potential in the bulk solution outside the membrane is equal to that just inside the membrane, expressed as

$$\overline{\mu}_{i_0} + RT \ln c_i + RT z_i \phi = \overline{\mu}_{m,i_0} + RT \ln c_{m,i} + RT z_i \phi_m \tag{21}$$

where $\overline{\mu}_{i0}$ is the chemical potential of the ion in the bulk solution at the membrane-solution interface, and $\overline{\mu}_{m,i_0}$ in the membrane at the same interface. Non-dimensionalizing Eq. (21) allows one to relate the concentrations at the membrane-solution interface using Boltzmann's law, given by

$$c^*_{m,i} = c_i \exp\left(-z_i \Delta\phi_D + \mu_i^{aff}\right) \tag{22}$$

where $c^*_{m,i}$ is the concentration of ions in the membrane at the membrane-solution interface, $\Delta\phi_D$ is the dimensionless Donnan potential at the membrane-solution interface and μ_i^{aff} is the ion affinity, which is a dimensionless term that describes the selectivity of a membrane towards specific ions. By substituting Eq. (22) into the electroneutrality equations for the membrane and the flow channels, Eq. (10) and Eq. (19), the Donnan potential can be calculated.

In the present study, the ED system was considered to be in equilibrium at $t = 0$. The system of differential equations was solved using the method of lines with variable step-size, where we discretized the equations with a fixed distance. The model input parameters, such as membrane characteristics, initial concentrations of the ions and system operational conditions were determined experimentally by characterizing the membranes and by conducting ED experiments.

3. Materials and methods

We characterized the ion exchange membranes for the parameters included in the developed theory, such as thickness, fixed charge density, membrane-water friction coefficient, ion affinity, and the diffusion coefficient reduction factor. Thereafter, we performed batch-mode ED experiments to study the removal of ions during operation, and the obtained data were used to validate the theoretical model.

3.1. Membrane characterization

Characterization experiments were conducted for homogenous Neosepta CMX-fg cation exchange membranes (Astom, Tokuyama Co., Japan) and AMX-fg anion exchange membranes (Astom, Tokuyama Co., Japan), and of each membrane properties such as thickness, fixed charge density and membrane-water friction coefficient were determined. Additionally, ion specific properties such as affinity and diffusion coefficient reduction factors were determined for Na^+ and K^+ ions. Before each characterization experiment, membrane samples were pre-soaked and stored in an 0.5 M NaCl solution for at least 24 h in order to have the same initial conditions. All experiments were performed at room temperature.

3.1.1. Thickness and water content

Membrane samples of 3 cm × 3 cm were soaked into 1 M NaCl solution for 24 h, and the wet weight of each sample was determined. The thickness of the membranes was measured at different spots with a disk micrometre (Mitutoyo, 369-511-30) and an average value was calculated. After that, the membrane samples were dried in a vacuum oven at 40 °C for 24 h to determine the dry weight. The water content of the membranes, u, was calculated by

$$u = \frac{m_{wet} - m_{dry}}{m_{dry}} \tag{23}$$

where m_{wet} and m_{dry} are the wet and dry weight (g) of the membrane samples, respectively.

3.1.2. Ion exchange capacity and fixed charge density

The fixed charge density and ion exchange capacity of each membrane were determined by analysing the concentration of counterions adsorbed by a membrane sample. Membrane samples of 5 cm × 5 cm were equilibrated in 0.5 M NaCl solution for 24 h to assure complete loading of membranes with counterions. Thereafter, the membrane samples were briefly soaked into demineralized water in order to remove excessive and absorbed solutions. After that, CEM samples were submerged into 0.5 M KCl solution to exchange all loaded Na^+ by K^+ ions, and AEM samples were submerged into 0.5 M $NaNO_3$ solution to exchange all loaded Cl^- ions by NO_3^- ions. Solutions for both membrane samples were renewed once, after 2 h, within 24 h. The submerge solutions of the same type of membrane were combined, and Na^+ and Cl^- concentrations in the final solutions were analysed using inductively coupled plasma spectrometry (ICP) and ion chromatography (IC) analyses, respectively. Finally, the membrane samples were dried in a vacuum oven at 40 °C for 24 h, and the dry weight was determined. The ion exchange capacity, *IEC* (mol·g_{dry}^{-1}), and fixed charge density, *X*, of the membranes were calculated using

$$IEC = \frac{c_{ct}\, V_{tot}}{M_{ct}\, m_{dry}} \tag{24}$$

$$X = \frac{IEC}{u} \tag{25}$$

where c_{ct} is the measured counterion concentration in the final solution, V_{tot} is the volume of the final solution and M_{ct} is the molecular weight of the counterion.

3.1.3. Membrane-water friction coefficient

Membrane-water friction coefficient, f_{w-m}, was determined by water permeability measurements through the membranes under an osmotic pressure difference. A two-chamber cell with a membrane of 8 cm^2 in between was used for the measurements. One of the chambers was filled with demineralized water and the other chamber was filled with 0.5 M NaCl solution in order to create an osmotic pressure difference across the membranes. The volume of water transported through the membranes with time was determined by measuring the water level change in the concentrate chamber. The conductivity of the solutions in both chambers were measured before and after the experiments in order to monitor the osmotic pressure change between the chambers. The average superficial water velocity, v_w, and the water permeability, L_p (ml·m^{-2}·bar^{-1}·hr^{-1}), were calculated using

$$v_w = \frac{V_t}{A\, t} \tag{26}$$

$$L_p = \frac{v_w}{\Delta P} \tag{27}$$

where V_t is the water volume transported, *A* is the membrane area, *t* is time and ΔP is the osmotic pressure difference between the chambers. After determining the experimental water velocity, the membrane-water friction coefficient f_{w-m} was calculated using Eq. (S5).

3.1.4. Ion affinity

Membrane ion affinity, μ_i^{aff}, measurements were performed by analysing the amount of individual ions loaded into a membrane sample in a mixture. The procedure followed to measure the ion affinity is similar to the ion exchange capacity experiments, with the exception that the membrane samples were submerged in 0.1 M nitrate salt solutions consisting of a mixture of two different cations, with varying compositions. The composition of the solutions is given in Table 1. The ion affinity of the CEM was evaluated for K^+ and Na^+ ions conducting two different sets of experiments. The first experiment is performed to define the affinity of a single target ion, Na^+ or K^+ (Salt I) in a mixture with H^+ ions (Salt II), and the second experiment is performed to define the individual affinity of Na^+ (Salt I) and K^+ (Salt II) ions in a mixture together.

Table 1
Composition of the solutions used for the ion affinity measurements.

Concentration of Salt I (M)	Concentration of Salt I (M)
0.90	0.10
0.88[a]	0.12[a]
0.86[a]	0.14[a]
0.75	0.25
0.50	0.50
0.25	0.75
0.10	0.90

[a] Additional concentrations were used for the experiments with H^+ ions.

For the first set of experiments, 10 cm × 10 cm membrane samples were submerged in a mixture of $H^+ + Na^+$ and $H^+ + K^+$ solutions in order to determine the affinity of the target ions over H^+ ions. Solutions were renewed once, after 2 h, within 24 h. Thereafter, the membrane samples were briefly soaked into demineralized water and thereafter submerged into 1 M NaCl solutions for 24 h. Solutions were renewed twice, after 2 and 19 h, and all the NaCl solutions were collected for each membrane sample. The final solutions were titrated with 0.1 M NaOH solution in order to determine the H^+ concentration. Finally, the weight of the membrane samples was determined after drying them in a vacuum oven at 40 °C for 24 h. The concentration of H^+ ions loaded into the membrane samples, c_{m,H^+}, was calculated using

$$c_{m,H^+} = \frac{c_{tit}\, V_{tit}}{m_{dry}\, u} \tag{28}$$

where c_{tit} is the concentration of the titrant and V_{tit} is the volume of the titrant used. The remaining fixed groups inside the membranes were considered to be occupied by the target ion, Na^+ or K^+, and the target ion concentration, $c_{m,t}$, in the membranes was calculated using

$$X = c_{m,H^+} + c_{m,t}. \tag{29}$$

For the second set of experiments, the membrane samples of 5 cm × 5 cm were submerged into a mixture of Na^+ and K^+ solutions, which were renewed twice, after 2 and 19 h, within 24 h. Thereafter, the membrane samples were briefly soaked into demineralized water, and then submerged into 0.1 M $Mg(NO_3)_2$ solution to exchange all loaded target ions with Mg^{2+}. Solutions were renewed once, after 2 h, within 24 h and were collected for each membrane sample. The Na^+ and K^+ concentrations in the final solutions were measured using ICP analysis. The dry weight of the membrane samples was determined after drying them in a vacuum oven at 40 °C for 24 h. The concentration of both target ions in the membranes was calculated by

$$c_{m,t} = \frac{c_t\, V_{tot}}{M_t\, m_{dry}\, u} \tag{30}$$

where c_t is the target ion concentration analysed by ICP, V_{tot} is the volume of the final solution and M_t is the molecular weight of the target ion.

3.1.5. Diffusion coefficient reduction factor

In order to calculate the diffusion coefficient reduction factors, $d_{r,i}$, of Na^+ and K^+ ions inside the CEM, the conductivity of the membrane was determined using a two-channel ED cell. The membrane area was 1 cm^2 and the distance between the electrodes is 1 cm $NaNO_3$ and KNO_3 solutions with concentrations between 0.002 and 1 M were used for the experiments. Membrane samples were soaked into the measuring solution for at least 24 h prior to measurements in order to allow

equilibration.

Electrical impedance spectroscopy (EIS) was used to measure the potential difference and impedance over the membrane, which allows to calculate the membrane resistance. A potentiostat (Iviumstat, The Netherlands) was used for the experiments, and the measurements were done in a high frequency range (10^2 Hz to 10^7 Hz) and with a current amplitude of 10 mA. The potential difference over the cell, including the membrane, was determined as combined resistance of the membrane and the bulk solution, R_{m+s}, and without the membrane as the resistance of the bulk solution, R_s. The membrane resistance, R_m (Ω), was calculated as the difference between these two resistances using

$$R_{m+s} = R_m + R_{s.} \tag{31}$$

Then, the conductivity of the membranes, K_m (mS·cm^{-1}), was calculated according to

$$K_m = \frac{\delta_{mem}}{R_m \ A_c} \tag{32}$$

where δ_{mem} is the membrane thickness and A_c is the membrane area in the cell. For homogeneous IEMs, the membrane conductivity can be related to the ion concentrations and diffusion coefficients inside the membranes using [44]

$$K_m = \frac{F^2}{RT}\left(z_{ct}^2 D_{ct} c_{m,ct} + z_{co}^2 D_{co} c_{m,co}\right) \tag{33}$$

where subscripts 'ct' and 'co' refer to counter and co-ions, and the concentrations of the ions in the membrane, $c_{m,ct}$ and $c_{m,co}$, were calculated considering the Donnan equilibrium and electroneutrality condition, by solving Eq. (10) and Eq. (22) for each ionic species. As previously discussed in Section 2.1, a reduction factor was used in this study to determine the diffusion coefficient of the ions inside the membrane based on the values in the bulk solution. By substituting Eq. (6) into Eq. (33), the diffusion coefficient reduction factor, $d_{r,i}$, can be calculated using the conductivity data directly by assuming that the reduction factor is the same for counter and co-ions. As the concentration of co-ions is very low in the membrane, the value of $d_{r,i}$ is almost completely determined by the counterions.

3.2. Electrodialysis experiments

A laboratory-scale ED setup (PCCell BED 1–3 Compact, PCA GmbH, Germany), consisting of an ED stack and three tanks to store diluate, concentrate and electrolyte solutions, was used for the experiments. The ED stack is equipped with a Pt–Ir coated titanium anode and a V4A steel cathode. The stack contains ten repeating cell pairs, each consisting of one AEM (AMX-fg), one CEM (CMX-fg) and a spacer between them to create concentrate and diluate flow channels. One additional AEM was added to the end of the stack to minimize cation transport between flow and electrolyte channels. The active membrane area in the stack was 80 mm × 80 mm. A power supply (Voltcraft PPS-16005) was connected to the electrodes to apply current through the stack. Additionally, the effluent of the cell passed a cooling system before returning to the reservoirs to keep the temperature constant throughout the experiments.

Experiments were performed using single salt (Na^+) and monovalent mixture ($Na^+ + K^+$) solutions in order to validate the developed model for different conditions. Solutions were prepared using demineralized water and reagent-grade nitrate (NO_3^-) salts with the following ion compositions.

- 0.2 M $NaNO_3$ at 10 and 15 V
- 0.1 M $NaNO_3$ & 0.1 M KNO_3 at 10 and 15 V

Experiments were performed in batch-mode operation and feed solutions with a starting volume of approximately 1.2 L were recirculated through the ED stack continuously at a flow rate 30 L·h^{-1}. Two different voltages were tested (10 V and 15 V) and the current was continuously monitored throughout the experiments. Conductivity, pH and temperature of the solution in each tank were measured and recorded continuously by a multi-parameter (Hach SensION + MM374). Also, the water level in each tank was manually recorded to quantify the water transport. In order to determine the concentration of each ion in the multi-ionic solutions, samples were collected periodically from each tank and were analysed using ICP. For the single salt solutions, the concentrations were determined using the conductivity data. All experiments were conducted at ~20 °C and continued until the diluate solution reached a conductivity lower than 50 μS·cm^{-1}.

4. Results and discussion

4.1. Membrane characterization

4.1.1. General properties of the membranes

General properties of the membranes determined by the characterization experiments are presented in Table 2. In general, the results are in good agreement with values reported in literature except for the ion exchange capacity of CMX-fg membranes. In the present study, we report the ion exchange capacity of CMX-fg membranes in terms of Na^+ ions, which could give a higher value compared to the H^+ ions due to the limited association of H^+ ions with the (weak) acid groups inside the membrane, which restricts the determination of total fixed surface groups of the membranes [45]. Additionally, the H^+ ion acceptor ability of sulfonic acid (–HSO_3^-) groups present in CMX-fg membranes is significantly lower than that of water molecules; thus, H^+ ions tend to bind to water molecules to form H_3O^+ instead of binding to the membranes [46], resulting in lower ion exchange capacity measurement compared to the Na^+ form for the membranes with sulfonic acid groups.

4.1.2. Ion affinity

Ion affinity of the CEM was determined for Na^+ and K^+ as individual ions (in a mixture with H^+ ions) and in mixtures together. The concentrations of individual ions inside the membrane were plotted as function of the concentrations in the bulk solution, and the experimental results were compared with theory. Theoretical lines were obtained using the electroneutrality condition in the membranes, Eq. (10), and Donnan equilibrium, Eq. (22); and the μ_i^{aff} term in the Donnan equation was fitted to the experimental data.

Obtained plots for ion affinity calculations are presented in Fig. 2. The affinity of H^+ was set to zero for both experiments to obtain the relative affinity, μ_i^{aff}, of K^+ and Na^+ compared to H^+. The theory describes the experimental data well with $\mu_{Na^+}^{aff} = 0.702$ and $\mu_{K^+}^{aff} = 0.968$ (Fig. 2), which indicates that the CMX-fg type membranes have higher affinity and selectivity towards K^+ ions over Na^+ ions. For CEMs with fixed sulfonic acid (-HSO_3^-) groups, including the CMX-fg type membranes, similar ion selectivity of K^+ over Na^+ has been reported by several studies [53,54]. Fig. 2C shows the selectivity of the CEM towards the target ions in a binary mixture. The values of μ_i^{aff} obtained for Na^+ and K^+ from the first set of experiments were used for the theoretical calculations, and the obtained theoretical lines describe the selectivity of the membrane towards Na^+ and K^+ ions in binary mixtures as well. For the experiments including the target ion and H^+, experimental data points at high H^+ concentrations (0.090 and 0.075 M) were far off from the theory (Fig. 2A and B). In theoretical calculations, the fixed charge density value evaluated in terms of Na^+ ions (Table 2) was used to determine the ion concentrations inside the membrane, and it was considered that all the available fixed charge is compensated by both ions effectively. However, lower H^+ concentrations were observed inside the membrane at relatively high H^+ concentrations in the bulk solution, due to the inability of H^+ ions to occupy all fixed charge groups of the membrane as explained in Section 4.1.1.

Table 2
Experimentally determined and literature values for general membrane properties. All experiments were repeated using two or three membrane samples, and the average values are reported.

	Neosepta, CMX-fg		Neosepta, AMX-fg	
	Measured values	Values in literature	Measured values	Values in literature
Thickness (mm)	0.145	0.140–0.200 [47]	0.158	0.120–0.180 [47]
Water content (wt%)	33.6	18 [45] 32 [48]	19.5	16 [45] 21 [48]
Ion exchange capacity (mmol·g_{dry}^{-1})	2.18	1.5–1.8 [47] 2.0[a] [49]	1.58	1.4–1.7 [47]
Fixed charge density (M)	6.51	6.30 [50] 9.00[a] [45]	8.19	7.81[b] [45] 7.93[b] [51]
Water permeability (ml·m^{-2}·bar^{-1}·hr^{-1})	4.94	2.5–6.5[c] [52]	2.95	2.0–6.5[c] [52]
Membrane-water friction (Tmol·s·m^{-5})	15	–	110	–

[a] Data reported based on exchange experiments with Na^+ ions.
[b] Calculated using the ion exchange capacity and the water content values reported in the study.
[c] Data are of membranes with similar properties from a different manufacturer (Fujifilm Membrane Technology).

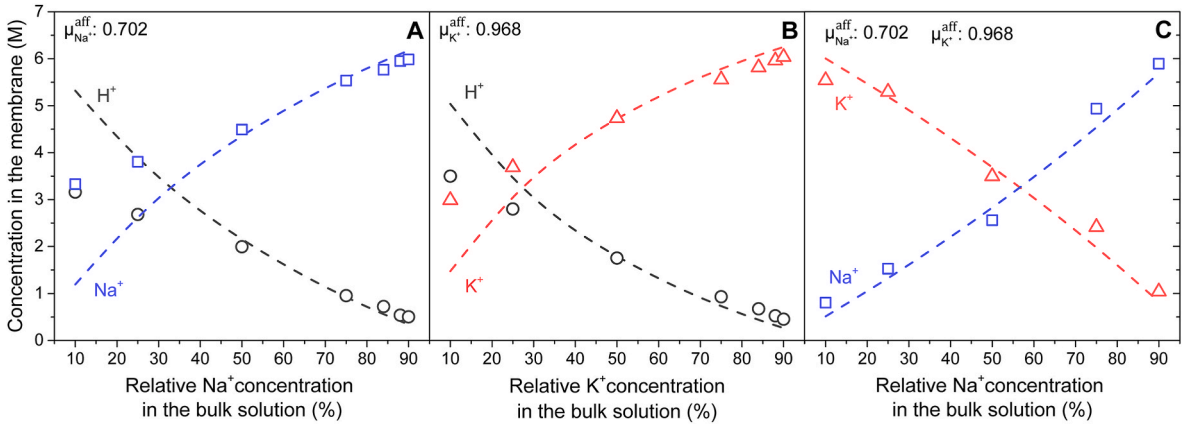

Fig. 2. Membrane affinity, μ_i^{aff}, of Na^+ over H^+ ions (A), of K^+ over H^+ ions (B), and of Na^+ and K^+ ions in a mixture (C). Markers: experimental data, dashed lines: theory.

4.1.3. Diffusion coefficient reduction factor

Diffusion coefficient reduction factors inside the CEM were determined for Na^+ and K^+ ions using the experimentally determined membrane conductivity data. The results of the resistance measurements as a function of ion concentration in bulk solution are given in Fig. S1 in the SI, and the calculated conductivity values from the resistance measurements are presented in Fig. 3. For both ions, the membrane resistance values were extremely high at bulk concentrations below 0.2 M and decreased rapidly with the bulk ion concentration (Fig. S1), indicating that at low salt concentrations the ionic charge inside the membrane is much lower, which is not correct. There is always a high concentration of counterions present inside the (ion exchange) membranes, because of the fixed membrane charge (Eq. (10) always holds). Therefore, the membrane conductivity should, especially at low salt concentrations, be close to independent of the bulk solution concentration. Comparable membrane conductivity results have been reported by several studies using similar experimental methods when the bulk solution concentration is low [55–59]. The main reason for low membrane conductivity values at low bulk concentrations is that at low bulk concentrations, the resistance in the bulk solution is extremely high and it dominates the total resistance [60,61]. As a result, large errors are expected in the resistance measurements at low bulk concentrations and subsequently in the calculation of the membrane conductivity as explained in Section 3.1.5.

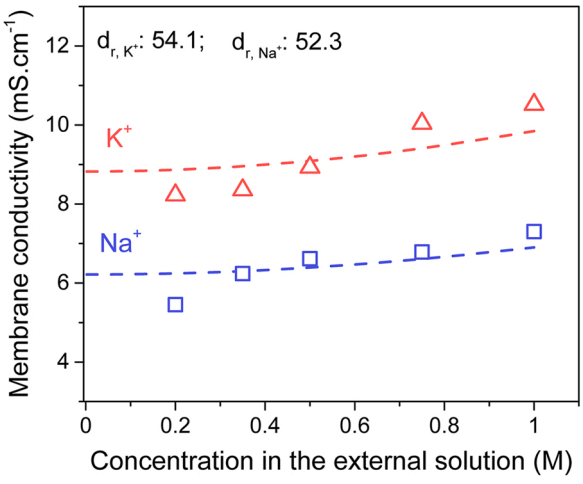

Fig. 3. Membrane conductivity values measured for single salt Na^+ and K^+ solutions at different external ion concentrations. Markers: experimental data, dashed lines: theory.

Kamcev et al. [60] have studied the effect of the bulk ion concentration on membrane resistance measurements by introducing an alternative direct measurement method. In their work, the resistance contribution of the bulk solution to the membrane resistance was aimed to be eliminated by submerging the membranes briefly into a solution with a high salt concentration just before the measurements. The study showed that when the resistance of the bulk solution is negligible, the membrane resistance values at external solutions with low concentrations are relatively constant, and the membrane conductivity increases slightly as a function of the co-ion concentration inside the membranes

[60], which also follows Eq. (33). The same behaviour was observed in the present study when the concentration of the bulk solution is above 0.2 M (Fig. 3). Therefore, the membrane conductivity data for the bulk concentration above 0.2 M were considered for $d_{r,i}$ calculation. Theory lines in Fig. 3 were obtained using Eq. (33), and $d_{r,i}$ terms were fitted to the experimental data using $d_{r,\mathrm{Na}}^{+} = 52.3$ and $d_{r,\mathrm{K}}^{+} = 54.1$. The obtained reduction factors are in line with the theoretical calculations reported by Biesheuvel and Dykstra (p. 135) [44].

The average membrane conductivity value obtained for K^+ solutions (~9.21) is considerably higher than for Na^+ solutions (~6.58), which is directly related to the mobility of ions inside the membranes. Previous studies investigated the conductivity of membranes in Na^+ and K^+ solutions and reported that K^+ ions penetrate faster in the membranes than Na^+ ions, due to the lower hydration energy and higher diffusion coefficient of K^+ ions [62,63]. Additionally, the difference in $d_{r,i}$ values calculated for Na^+ and K^+ ions also suggests that the mobility of ions inside the membrane is not only affected by the physical properties of the membranes and the ions, but also by the specific ion-membrane interactions. We show that K^+ ions have stronger interactions (affinity) with the membrane charged groups in Section 4.1.2, which creates an additional resistance, and decreases the mobility of K^+ ions inside the membrane even more than of Na^+ ions.

4.2. Electrodialysis experiments: model validation

The validation of the model has been done for single salt solutions and monovalent mixtures using the data from the ED experiments considering different parameters, such as ion concentration, ionic flux, and water transport. The experiments were performed at constant voltage (10 V and 15 V), and the time-dependent experimental current density (Fig. S2 in the SI) was used as an input to the model for each experiment as in Eq. (12). The model input parameters used for the theoretical calculations were given in Table S1 in the SI.

4.2.1. Ion transport

The theory was validated for ion transport using the concentration and flux data. Experimental fluxes were calculated by dividing the ion concentration decrease in diluate channel by membrane area and time interval between the measurements. Changes in diluate and concentrate volume due to water transport were taken into account for the flux calculations.

For the single salt experiments, the theory described the experimental results well in the diluate and concentrate for Na^+ concentration, and Na^+ flux for both conditions (Fig. S3 in the SI). Next, we validate the theory with the data from the experiments with binary mixtures containing Na^+ and K^+, and the results are presented in Fig. 4. In general, the theoretical data describe the experimental data of the ionic fluxes and ionic concentrations well in the diluate. However, the K^+ flux through the concentrate channel was approximately 27% overestimated in the beginning of both experiments (Fig. 4B and D insets). Initial conditions of the theory may vary from the actual initial conditions in the experiments as the membranes may not be at equilibrium yet at the

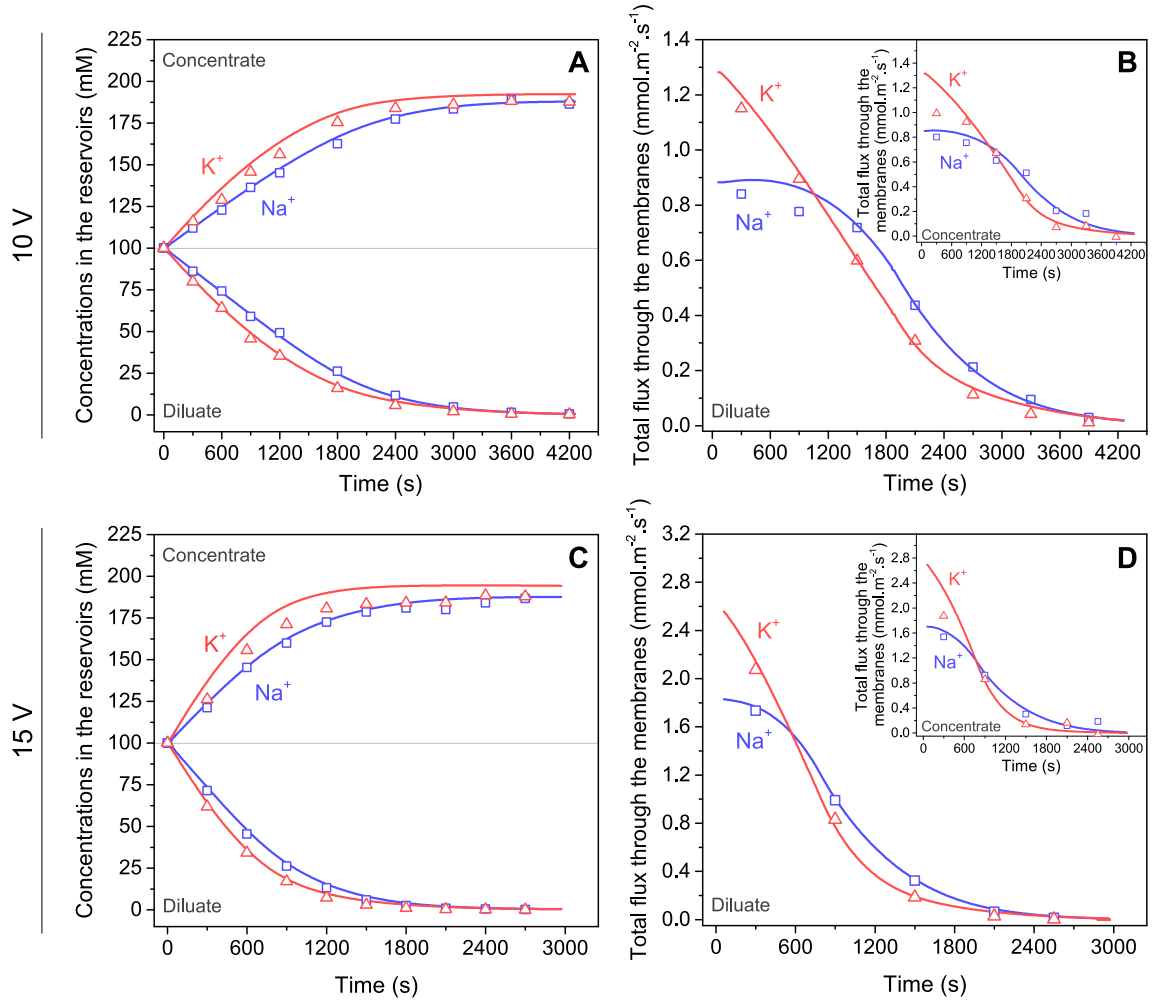

Fig. 4. Validation of the model for ED experiments with Na^+ and K^+ mixtures at 10 V and 15 V. Change of Na^+ and K^+ concentrations in the reservoirs (A, C), and Na^+ and K^+ flux through the membranes (B, D). Markers: experimental data, lines: model predictions.

start of the measurements, which could cause an overestimation observed in the beginning of the experiments for the ionic flux. Although the ionic flux predictions for the rest of the experiments are accurate, the accumulative effect of the ionic flux on the concentration change results in the overestimation of the concentration of K^+ ions in the concentrate by approximately 2.5% for 10 V (Fig. 4A) and 3.4% for 15 V (Fig. 4C) at the end of the experiments. The results also show a decrease of preferential transport of K^+ over Na^+ in time, this change will be discussed further in detail in Section 4.3 relating to the different ion transport mechanisms.

4.2.2. Water transport

Theoretical predictions for the water transport through membranes were also validated to evaluate ion transport by convection, as in Eq. (8). The results of the water transport for the experiments at 10 V are presented in Fig. 5A and B; the data for the experiments at 15 V can be found in Fig. S4 in the SI. The theoretical water flow was calculated by multiplying the water velocity (Eq. (S5)) through the membranes with the active membrane area in the ED stack.

In general, the theory is in agreement with the experimental water flow data and describes the trends that are experimentally observed (Fig. 5) with small discrepancies. In the theory, only the diluate and concentrate channels were included, and the water transport is considered between these two flow channels due to the friction between the ions and the water molecules, and the osmotic pressure difference. The experimental inaccuracies and the fluctuations in the measurements due to water oxidation/reduction at the electrodes and water being transported to/from the electrolyte channels was not considered in the theory, which could lead the observed discrepancies.

4.3. Model output: contribution of ion transport mechanisms to preferential ion removal

After validating the model for monovalent mixtures, we analyse the contribution of different mechanisms to ion transport. As previously mentioned in Section 2, ion transport inside the membranes is described by the three mechanisms: convection, diffusion and electromigration (Eq. (8)). Evaluating the contribution of each mechanism on individual ion transport is important to provide a more detailed understanding of the system selectivity. In the present study, we have studied the change in the contribution of different mechanisms on ion transport over time for Na^+ and K^+ in a mixture and the obtained results of the model at 10 V are shown in Fig. 6, at 15 V are given in Fig. S5 in the SI.

The electromigrative term has the largest contribution to the total Na^+ and K^+ transport in the beginning of both experiments due to the high current density. At the start of each experiment, the contribution of electromigration and convection mechanisms to transport of K^+ ions is higher than of Na^+ ions (Fig. 6A and B) due to the higher concentrations inside the membranes (Fig. 6C), which are a result of the higher affinity of K^+ ions, which leads to higher total flux and thus the selectivity for K^+ ions over Na^+ ions. While electromigration and convection decrease rapidly for both ions with time; the contribution of diffusion increases with the increasing concentration gradient over the membrane over time (Fig. 6C) and shows opposite trends for Na^+ and K^+ ions. The reason for that is the Donnan equilibrium, Eq. (22), which results in higher K^+ concentrations inside the membranes than Na^+ concentrations due to the higher affinity of K^+ (Fig. 6C, $t = 0$). When the electrical potential difference was applied to the ED stack, a negative concentration gradient was created for K^+ ions because of the concentration differences between concentrate and the diluate channels. In order to maintain electroneutrality in the system, Eq. (10), the concentration gradient of Na^+ ions is in the opposite direction, which has a positive contribution of diffusion on the Na^+ flux.

Here it can be concluded that the higher membrane affinity towards K^+ ions has two major effects on the transport of both ions: the first one is increasing the concentration of K^+ ions inside the membrane, thus enhancing electromigration and convection for K^+ ions; and the second one is creating a concentration gradient for Na^+ ions from the diluate side of the membrane to the concentrate side, and as a result enhancing diffusion of Na^+ ions. The effect of the opposite trends of diffusive transport on selectivity can be clearly observed in the first 600 s. Even though the flux of K^+ ions is considerably higher than the flux of Na^+ ions in the beginning of the experiments, with time the K^+ flux decreases rapidly while the Na^+ flux stays relatively constant, since the increasing diffusive transport of Na^+ ions compensates the decrease in electromigrative and convective transport, making the Na^+ flux more significant. Electromigration and convection are the mechanisms that favor K^+ transport during the wholeoperational period due to its ion properties, such as high affinity and high diffusion coefficient inside the membranes. On the other hand, diffusion is the main mechanism that controls and reverses the preferential ion transport (selectivity) in the system by oppositely contributing to the transport of K^+ and Na^+ ions especially

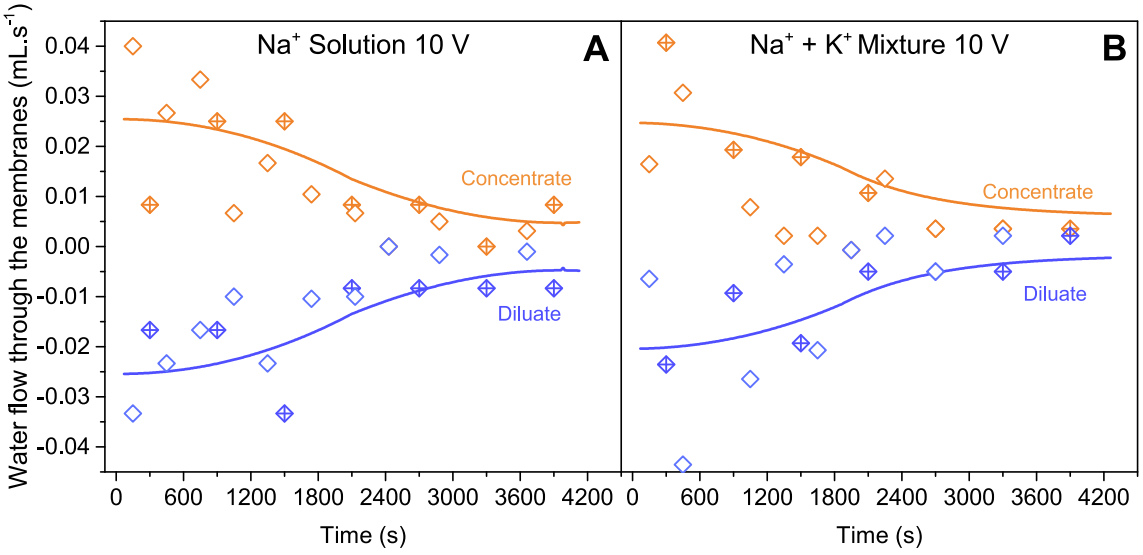

Fig. 5. Validation of the model for water flow through the membranes from the diluate channels to the concentrate channels in the ED stack; for the single Na^+ solution (A) and for Na^+ and K^+ mixture (B) at 10 V. Markers: experimental data of two desalination experiments, each indicated by a different marker, solid lines: model predictions.

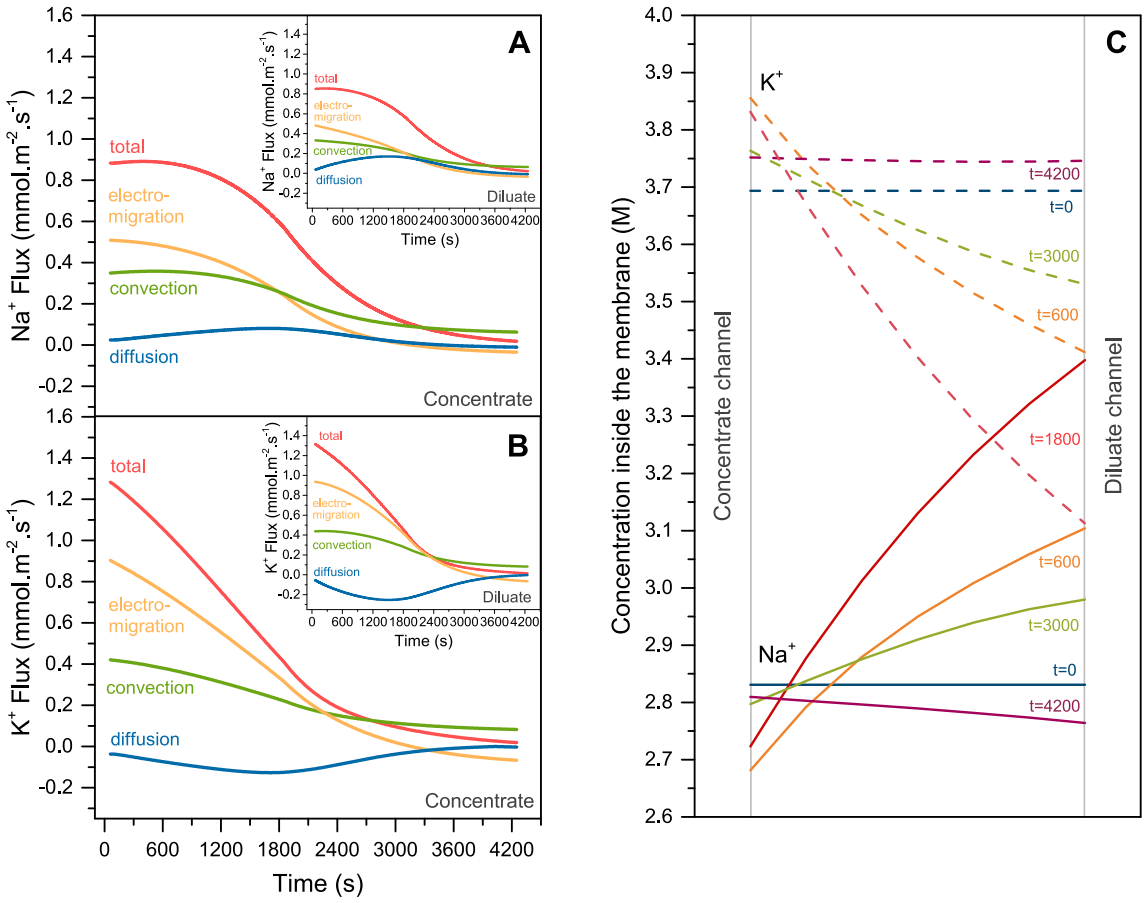

Fig. 6. Theoretical calculations of the relative contributions of convection, diffusion and electromigration mechanisms to the transport of Na^+ (A) and K^+ (B) through the membranes, and the concentration profiles of Na^+ and K^+ ions in the CEM at various times (t) during the operation (C). The data is presented for Na^+ and K^+ mixture at 10 V.

after 600 s in 10 V (Fig. 6) and after 900 s in 15 V experiments (Fig. S5). The effect of diffusion mechanism on individual ion fluxes can be found in Fig. S6 in the SI.

Another important aspect to note is the contribution of convection to ion transport through the membranes. In ED the leading transport mechanisms are considered as electromigration and diffusion, and convection due to water transport has been neglected in most of the studies. However, the results of the present study showed that convection contributes to ~ 35% of the total ionic flux in the ED system, and should be considered in theoretical calculations, especially to describe (selective) desalination of multi-ionic electrolyte solutions.

5. Conclusions

In the present study, a theoretical model for multicomponent mass transport in electrodialysis (ED) was developed based on the extended Nernst-Planck equation including water transport and ion-membrane frictions to investigate the selective transport of Na^+ and K^+ ions. Properties of the ion exchange membranes used in the ED stack were experimentally determined and included in the model. The selectivities of the cation exchange membranes (Neosepta CMX-fg) towards K^+ ions over Na^+ ions were determined experimentally by conducting adsorption and membrane conductivity measurements, and the obtained data was used to implement membrane selectivity into the model. Subsequently, the developed model was successfully validated for the concentration and flux of the ions, and the water transport using the data obtained by ED experiments for single salt solutions and multi-ionic mixtures. Additionally, a theoretical analysis was performed to evaluate the contributions of different ion transport mechanisms (electromigration, convection and diffusion) on individual transport of Na^+ and K^+ ions in ED, and their role in selective transport was investigated. The results showed that, even though electromigration has the highest contribution to the ionic flux for both Na^+ and K^+ ions, diffusion is the main mechanism that could control or switch the selective ion transport in ED due to its opposite contribution to Na^+ and K^+ ions. Moreover, convective transport driven by water transport contributes to approximately 35% of the total ion flux for both Na^+ and K^+ ions in ED, and it is important to include water transport in theoretical and practical studies.

Author statement

The manuscript was written through contributions of all authors. All authors have given approval to the final version of the manuscript.

Declaration of competing interest

The authors declare that they have no known competing financial interests or personal relationships that could have appeared to influence the work reported in this paper.

Data availability

Data will be made available on request.

Acknowledgements

This project was funded by the Dutch Topsector AgriFood “Natte

Stromen" (DFI-AF-18003).

Appendix A. Supplementary data

Supplementary data to this article can be found online at https://doi.org/10.1016/j.memsci.2022.121114.

References

[1] D. Fatta-Kassinos, D.D. Dionysiou, K. Kümmerer, Wastewater Reuse and Current Challenges, Springer International Publishing, 2016.
[2] Y.D. Ahdab, G. Schucking, R. Danyal, J.H. Lienhard, Treatment of greenhouse wastewater for reuse or disposal using monovalent selective electrodialysis, Desalination 507 (2021) 115037.
[3] G.J. Doornbusch, M. Tedesco, J.W. Post, Z. Borneman, K. Nijmeijer, Experimental investigation of multistage electrodialysis for seawater desalination, Desalination 464 (2019) 105–114.
[4] A.-A. Sajjad, M.Y.B.M. Yunus, A.A.M. Azoddein, D.G. Hassell, I.H. Dakhil, H. A. Hasan, Electrodialysis desalination for water and wastewater: a review, Chem. Eng. J. 380 (2019) 122231.
[5] F. Valero, A. Barceló, R. Arbós, Electrodialysis Technology - Theory and Applications, Desalination, Trends and Technologies, InTech, 2011.
[6] Z. Zourmand, F. Faridirad, N. Kasiri, T. Mohammadi, Mass transfer modeling of desalination through an electrodialysis cell, Desalination 359 (2015) 41–51.
[7] M. Sadrzadeh, A. Kaviani, T. Mohammadi, Mathematical modeling of desalination by electrodialysis, Desalination 206 (2007) 538–546.
[8] F.S. Rohman, M.R. Othman, N. Aziz, Modeling of batch electrodialysis for hydrochloric acid recovery, Chem. Eng. J. 162 (2010) 466–479.
[9] A. Campione, L. Gurreri, M. Ciofalo, G. Micale, A. Tamburini, A. Cipollina, Electrodialysis for water desalination: a critical assessment of recent developments on process fundamentals, models and applications, Desalination 434 (2018) 121–160.
[10] T.M. Mubita, S. Porada, P.M. Biesheuvel, A. van der Wal, J.E. Dykstra, Strategies to increase ion selectivity in electrodialysis, Separ. Purif. Technol. 292 (2022) 120944.
[11] Y. Kim, W.S. Walker, D.F. Lawler, Competitive separation of di- vs. mono-valent cations in electrodialysis: effects of the boundary layer properties, Water Res. 46 (2012) 2042–2056.
[12] A.H. Galama, G. Daubaras, O.S. Burheim, H.H.M. Rijnaarts, J.W. Post, Seawater electrodialysis with preferential removal of divalent ions, J. Membr. Sci. 452 (2014) 219–228.
[13] P.A. Sosa-Fernandez, J.W. Post, A.M. Leermakers, H.H.M. Rijnaarts, H. Bruning, Removal of divalent ions from viscous polymer-flooding produced water and seawater via electrodialysis, J. Membr. Sci. 589 (2019) 117251.
[14] A.M. Benneker, J. Klomp, R.G.H. Lammertink, J.A. Wood, Influence of temperature gradients on mono- and divalent ion transport in electrodialysis at limiting currents, Desalination 443 (2018) 62–69.
[15] M. Reig, H. Farrokhzad, B. Van der Bruggen, O. Gibert, J.L. Cortina, Synthesis of a monovalent selective cation exchange membrane to concentrate reverse osmosis brines by electrodialysis, Desalination 375 (2015) 1–9.
[16] X. Pang, Y.Y. Tao, Y.Q. Xu, J.F. Pan, J.N. Shen, C.J. Gao, Enhanced monovalent selectivity of cation exchange membranes via adjustable charge density on functional layers, J. Membr. Sci. 595 (2020) 117544.
[17] B. Cohen, N. Lazarovitch, J. Gilron, Upgrading groundwater for irrigation using monovalent selective electrodialysis, Desalination 431 (2018) 126–139.
[18] X.S. Xu, Q. He, G.Y. Ma, H.Y. Wang, N. Nirmalakhandan, P. Xu, Selective separation of mono- and di-valent cations in electrodialysis during brackish water desalination: bench and pilot-scale studies, Desalination 428 (2018) 146–160.
[19] T. Sata, T. Yamaguchi, K. Matsusaki, Effect of hydrophobicity of ion-exchange groups of anion-exchange membranes on permselectivity between two anions, J. Phys. Chem. 99 (1995) 12875–12882.
[20] Y. Li, T.W. Xu, Permselectivities of monovalent anions through pyridine-modified anion-exchange membranes, Separ. Purif. Technol. 61 (2008) 430–435.
[21] T. Mubita, S. Porada, P. Aerts, A. van der Wal, Heterogeneous anion exchange membranes with nitrate selectivity and low electrical resistance, J. Membr. Sci. 607 (2020) 118000.
[22] Z.X. Qian, H. Miedema, S. Sahin, L.C.P.M. de Smet, E.J.R. Sudholter, Separation of alkali metal cations by a supported liquid membrane (SLM) operating under electro dialysis (ED) conditions, Desalination 495 (2020), 114631.
[23] S.S. Yang, Y.W. Liu, J.B. Liao, H.W. Liu, Y.L. Jiang, B. Van der Bruggen, J.N. Shen, C.J. Gao, Codeposition Modification of cation exchange Membranes with Dopamine and crown ether to achieve high K^+ electrodialysis selectivity, ACS Appl. Mater. Interfaces 11 (2019) 17730–17741.
[24] G. Kraaijeveld, V. Sumberova, S. Kuindersma, H. Wesselingh, Modeling electrodialysis using the maxwell-stefan description, Chem. Eng. J. Biochem. Eng. J. 57 (1995) 163–176.
[25] C. Delacourt, J. Newman, Mathematical modeling of a cation-exchange membrane containing two cations, J. Electrochem. Soc. 155 (2008) B1210–B1217.
[26] R.R. Sijabat, M.T. de Groot, S. Moshtarikhah, J. van der Schaaf, Maxwell-Stefan model of multicomponent ion transport inside a monolayer Nafion membrane for intensified chlor-alkali electrolysis, J. Appl. Electrochem. 49 (2019) 353–368.
[27] J.A. Hogendoorn, A.J. van der Veen, J.H.G. van der Stegen, J.A.M. Kuipers, G. F. Versteeg, Application of the Maxwell-Stefan theory to the membrane electrolysis process - model development and simulations, Comput. Chem. Eng. 25 (2001) 1251–1265.
[28] E.E. Graham, J.S. Dranoff, Application of the stefan-maxwell equations to diffusion in ion-exchangers .1. Theory, Ind. Eng. Chem. Fundam. 21 (1982) 360–365.
[29] C.M. Silva, P.F. Lito, Application of the Maxwell-Stefan approach to ion exchange in microporous materials. Batch process modelling, Chem. Eng. Sci. 62 (2007) 6939–6946.
[30] K. Tado, F. Sakai, Y. Sano, A. Nakayama, An analysis on ion transport process in electrodialysis desalination, Desalination 378 (2016) 60–66.
[31] M. Tedesco, H.V.M. Hamelers, P.M. Biesheuvel, Nernst-Planck transport theory for (reverse) electrodialysis: I. Effect of co-ion transport through the membranes, J. Membr. Sci. 510 (2016) 370–381.
[32] M. Tedesco, H.V.M. Hamelers, P.M. Biesheuvel, Nernst-Planck transport theory for (reverse) electrodialysis: II. Effect of water transport through ion-exchange membranes, J. Membr. Sci. 531 (2017) 172–182.
[33] Y. Tanaka, Concentration polarization in ion-exchange membrane electrodialysis - the events arising in a flowing solution in a desalting cell, J. Membr. Sci. 216 (2003) 149–164.
[34] V. Fila, K. Bouzek, A mathematical model of multiple ion transport across an ion-selective membrane under current load conditions, J. Appl. Electrochem. 33 (2003) 675–684.
[35] V.I. Zabolotsky, J.A. Manzanares, V.V. Nikonenko, K.A. Lebedev, E.G. Lovtsov, Space charge effect on competitive ion transport through ion-exchange membranes, Desalination 147 (2002) 387–392.
[36] Y. Yang, P.N. Pintauro, Multicomponent space-charge transport model for ion-exchange membranes with variable pore properties, Ind. Eng. Chem. Res. 43 (2004) 2957–2965.
[37] P.M. Biesheuvel, S. Porada, M. Elimelech, J.E. Dykstra, Tutorial review of reverse osmosis and electrodialysis, J. Membr. Sci. 647 (2022) 120221.
[38] W.M. Deen, Hindered transport of large molecules in liquid-filled pores, AIChE J. 33 (1987) 1409–1425.
[39] T. Luo, S. Abdu, M. Wessling, Selectivity of ion exchange membranes: a review, J. Membr. Sci. 555 (2018) 429–454.
[40] J.E. Dykstra, A. ter Heijne, S. Puig, P.M. Biesheuvel, Theory of transport and recovery in microbial electrosynthesis of acetate from CO_2, Electrochim. Acta 379 (2021) 138029.
[41] A.N. Shocron, E.N. Guyes, H.H.M. Rijnaarts, P.M. Biesheuvel, M.E. Suss, J. E. Dykstra, Electrochemical removal of amphoteric ions, Proc. Natl. Acad. Sci. U.S. A. 118 (2021), e2108240118.
[42] R. Ronen, I. Atlas, M.E. Suss, Theory of flow batteries with fast homogeneous chemical reactions, J. Electrochem. Soc. 165 (2018) A3820–A3827.
[43] F.G. Donnan, The theory of membrane equilibria, Chem. Rev. 1 (1924) 73–90.
[44] P.M. Biesheuvel, J.E. Dykstra, Physics of Electrochemical Processes, 2020.
[45] P. Dlugolecki, K. Nymeijer, S. Metz, M. Wessling, Current status of ion exchange membranes for power generation from salinity gradients, J. Membr. Sci. 319 (2008) 214–222.
[46] I.A. Stenina, A.B. Yaroslavtsev, Ionic mobility in ion-exchange membranes, Membranes 11 (2021) 198.
[47] T.W. Xu, Ion exchange membranes: state of their development and perspective, J. Membr. Sci. 263 (2005) 1–29.
[48] D. Pintossi, C.L. Chen, M. Saakes, K. Nijmeijer, Z. Borneman, Influence of sulfate on anion exchange membranes in reverse electrodialysis, Nat. Prod. J.Clean Water 3 (2020) 29.
[49] M. Higa, M. Nishimura, K. Kinoshita, A. Jikihara, Characterization of cation-exchange membranes prepared from poly(vinyl alcohol) and poly(vinyl alcohol-b-styrene sulfonic acid), Int. J. Hydrogen Energy 37 (2012) 6161–6168.
[50] A.H. Avci, T. Rijnaarts, E. Fontananova, G. Di Profio, I.F.V. Vankelecom, W.M. De Vos, E. Curcio, Sulfonated polyethersulfone based cation exchange membranes for reverse electrodialysis under high salinity gradients, J. Membr. Sci. 595 (2020) 117585.
[51] P. Dlugolecki, P. Ogonowski, S.J. Metz, M. Saakes, K. Nijmeijer, M. Wessling, On the resistances of membrane, diffusion boundary layer and double layer in ion exchange membrane transport, J. Membr. Sci. 349 (2010) 369–379.
[52] Ion Exchange Membranes for Water Purification, Product Brochure. Fujifilm Membrane Technology: The Netherlands.
[53] H. Strathmann, Ion-exchange membrane separation processes, in: Membrane Science and Technology Series, first ed., Elsevier. xi, Amsterdam ; Boston, 2004, p. 348.
[54] A. Chaabouni, F. Guesmi, I. Louati, C. Hannachi, B. Hamrouni, Temperature effect on ion exchange equilibrium between CMX membrane and electrolytes solutions, J. Water Reuse Desalination 5 (2015) 535–541.
[55] A.H. Galama, D.A. Vermaas, J. Veerman, M. Saakes, H.H.M. Rijnaarts, J.W. Post, K. Nijmeijer, Membrane resistance: the effect of salinity gradients over a cation exchange membrane, J. Membr. Sci. 467 (2014) 279–291.
[56] P. Dlugolecki, B. Anet, S.J. Metz, K. Nijmeijer, M. Wessling, Transport limitations in ion exchange membranes at low salt concentrations, J. Membr. Sci. 346 (2010) 163–171.
[57] T. Luo, F. Roghmans, M. Wessling, Ion mobility and partition determine the counter-ion selectivity of ion exchange membranes, J. Membr. Sci. 597 (2020) 117645.
[58] J.H. Choi, S.H. Kim, S.H. Moon, Heterogeneity of ion-exchange membranes: the effects of membrane heterogeneity on transport properties, J. Colloid Interface Sci. 241 (2001) 120–126.
[59] F.Q. Mir, A. Shukla, Sharp rise in resistance of ion exchange membranes in low concentration NaCl solution, J. Taiwan Inst. Chem. Eng. 72 (2017) 134–141.

[60] J. Kamcev, R. Sujanani, E.S. Jang, N. Yan, N. Moe, D.R. Paul, B.D. Freeman, Salt concentration dependence of ionic conductivity in ion exchange membranes, J. Membr. Sci. 547 (2018) 123–133.
[61] J.C. Diaz, J. Kamcev, Ionic conductivity of ion-exchange membranes: measurement techniques and salt concentration dependence, J. Membr. Sci. 618 (2021) 118718.
[62] V.K. Shahi, A.P. Murugesh, B.S. Makwana, S.K. Thampy, R. Rangarajan, Comparative investigations on electrical conductance of ion-exchange membranes, Indian J. Chem. Sect. A Inorg. Bio-Inorg. Phys. Theor. Anal. Chem. 39 (2000) 1264–1269.
[63] T. Ojala, K. Kontturi, Transport-properties of a cation-exchange membrane with sodium and potassium as counterions, Acta Chem. Scand. 43 (1989) 340–344.